

Evaluation of the intra- and inter-method agreement of brain MRI segmentation software packages: a comparison between SPM12 and FreeSurfer v6.0

L. Palumbo¹, P. Bosco¹, M.E. Fantacci², E. Ferrari^{1,3}, P. Oliva⁴, G. Spera¹, A. Retico¹

¹National Institute for Nuclear Physics (INFN), Pisa Division, Pisa, IT

²University of Pisa, Physics Department, Pisa, IT

³Scuola Normale Superiore, Pisa, IT

⁴University of Sassari and INFN Cagliari Division, IT

Abstract

Purpose

The lack of inter-method agreement can produce inconsistent results in neuroimaging studies. We evaluated the intra-method repeatability and the inter-method reproducibility of two widely-used automatic segmentation methods for brain MRI: the FreeSurfer (FS) and the Statistical Parametric Mapping (SPM) software packages.

Methods

We segmented the gray matter (GM), the white matter (WM) and subcortical structures in test-retest MRI data of healthy volunteers from Kirby-21 and OASIS datasets. We used Pearson's correlation (r), Bland-Altman plot and Dice index to study intra-method repeatability and inter-method reproducibility. In order to test whether different processing methods affect the results of a neuroimaging-based group study, we carried out a statistical comparison between male and female volume measures.

Results

A high correlation was found between test-retest volume measures for both SPM (r in the 0.98-0.99 range) and FS (r in the 0.95-0.99 range). A non-null bias between test-retest FS volumes was detected for GM and WM in the OASIS dataset. The inter-method reproducibility analysis measured volume correlation values in the 0.72-0.98 range and the overlap between the segmented structures assessed by the Dice index was in the 0.76-0.83 range. SPM systematically provided significantly greater GM volumes and lower WM and subcortical volumes with respect to FS. In the male vs. female brain volume comparisons, inconsistencies arose for the OASIS dataset, where the gender-related differences appear subtler with respect to the Kirby dataset.

Conclusions

The inter-method reproducibility should be evaluated before interpreting the results of neuroimaging studies.

Keywords: brain MRI, segmentation, repeatability, reproducibility

Introduction

In the last 20 years, magnetic resonance imaging (MRI) has allowed to non-invasively study brain structure at high resolutions. In neuroscience research, segmenting a brain MRI into different structures is a widely used pre-processing step [1,2]. Even though the manual segmentation is considered the gold standard [3], it is operator-dependent, laborious, and time-consuming. Automated segmentation tools are used to segment the brain regions in a reasonable

1 amount of time and thus they are essential for investigating large datasets. These automatic methods have been used in a
2 large number of research studies on psychiatric and neurological disorders. However, the reliability of their
3 measurements is a matter of debate [4], in terms of both reproducibility and repeatability. The reproducibility is the
4 measure of agreement between the results obtained with the two methods on the same scan of a subject. The
5 repeatability is the degree of agreement between brain volumes obtained with the same method on an identical subject
6 in two subsequent acquisitions (test-retest analysis).
7

8 Several studies [4–7] focused on the test-retest repeatability assessment of automatic segmentation methods. For
9 example, Chard et al. [5] investigated the repeatability of gray matter (GM) and white matter (WM) volumes obtained
10 with the Statistical Parametric Mapping (SPM) software package, showing that SPM99 was reliable to segment GM and
11 WM, with Pearson’s correlations of 0.908 and 0.895, respectively. In addition, they showed that the inhomogeneity
12 correction improves the repeatability. Several studies reported high inter-method reproducibility between automatic
13 segmentation methods, but some of them highlight the presence of method-specific biases [6–12]. In fact, processing
14 methods can systematically either underestimate or overestimate the volumes of different brain regions with respect to a
15 reference volume, defined for instance by manual segmentation. Relevant differences between SPM and FreeSurfer
16 (FS) were shown by Katuwal et al. [8] in the estimated GM and WM volumes. In that case, the volumes obtained with
17 SPM8 were closer to manual segmentations than those obtained with FS v5.3; in particular, SPM8 overestimated GM
18 and WM volumes with respect to FS v5.3, by 40% and 26%, respectively. In the study by Wenger et al. [9], FS v5.3
19 was shown to overestimate the hippocampal volume with respect to manual segmentation. However, even though
20 Kazemi et al. [10] showed the superior accuracy of SPM8 in segmenting brain tissues with respect to other automated
21 methods, they also pointed out that it is not suitable for the segmentation of subcortical structures. Perlaki et al. [13]
22 showed that FS v4.5/v5.3 was less accurate in the segmentation of putamen with respect to FSL-FIRST. The
23 discrepancies in volume estimates between different segmentation algorithms could reside in the different image
24 processing algorithms implemented (e.g. the use of different templates and image registration methods) [8].
25

26 The reliability of automatic segmentation methods and the comparison between automated segmentation software
27 packages has been evaluated in various studies [14–16]. A summary of structural MRI studies on the repeatability of
28 automatic segmentation software is reported in Table 1, together with the investigated brain regions and used methods.
29

30 In this work we provide a direct and appropriate comparison between the latest versions of the software packages of
31 two popular segmentation methods, Statistical Parametric Mapping (v12) [17,18] and FreeSurfer (v6.0) [19,20], using
32 two publicly available datasets, namely Kirby [21] and OASIS [22].
33

34 The aim of this work is to analyze the intra-method repeatability, the inter-method reproducibility and the possible
35 systematic bias in the volume estimates generated by the two automatic segmentation software, focusing on six regions
36 of interest (ROIs): two global measures (GM and WM) and four subcortical structures (hippocampus, putamen, caudate
37 and brainstem). The reliability of each method and the quantification of any discrepancy are relevant for the correct
38 interpretation of the results of longitudinal studies and for quantitative considerations in meta-analyses.
39

40 In order to test how the use of different segmentation algorithms could affect the results of volume group comparisons,
41 we analyzed the differences in brain volume measures between male and female subgroups in both OASIS and Kirby
42 data samples, using SPM12 and FS v6.0.
43
44
45
46
47
48
49
50
51
52
53
54
55
56
57
58
59
60
61
62
63
64
65

Materials and Methods

Data samples

We examined two publicly available data samples: the Kirby-21 (Kirby) dataset [21,23], and the OASIS dataset [22,24]. The Kirby dataset consists of 3D T1-weighted images of 21 healthy volunteers (11 males and 10 females; age: 32 ± 9 years) that were acquired using a 3T MRI scanner. The acquisition protocol included whole-brain high-resolution anatomical 3D images (MPRAGE sequence, TE/TR 6.7/3.1 ms, $1 \times 1 \times 1.2$ mm voxel size, flip angle 8°). For repeatability studies, MRI images were acquired twice: after the first session, each subject left the scan room for a short break and then he/she was repositioned in the scanner for an identical session with the same acquisition parameters [21].

The OASIS dataset consists of 3D T1-weighted images of 20 healthy volunteers (8 males and 12 females; age: 23.4 ± 3.9 years), acquired using a 1.5 T MRI scanner. The acquisition protocol included a whole-brain high-resolution anatomical scan (MPRAGE sequence, TE/TR 4.0/9.7 ms, $1 \times 1 \times 1$ mm voxel size, flip angle 10°) [16,25]. The 20 subjects were scanned twice with a time delay in the range of 1-89 days (mean delay of about 21 days) to enable repeatability studies [22,25].

An example of anatomical scans of two datasets is shown in Fig.1.

The test-retest analysis allows estimating a tool's reliability in measuring a given quantity in the successive repetition of the measurement under the same conditions. MRI data may be affected by confounding factors that may vary between scans, like the field of view, or patient positioning. In addition, there are effects such as hydration levels that cause possible day-to-day variations in the brain structures [4,26].

Segmentation and volume measures

We estimated the volumes of six different brain tissues: GM, WM and four subcortical structures (hippocampus, putamen, caudate and brainstem), using two processing methods: FS v6.0 and SPM12. Both FS and SPM are a set of tools and algorithms to extract measures from neuroimaging data for the study of the human brain in healthy and pathological conditions.

FreeSurfer is used as a pre-processing workflow for structural MRI data (recon-all analysis pipeline) [19], which performs all cortical reconstruction through 31 processing steps. The FS pipeline is shown in Fig. 2(a).

To carry out brain tissue segmentation, FS takes advantage of a lot of information, e.g. image intensities, global position within the brain and position relative to neighboring brain structures. Then, it uses probabilistic atlas in which coordinates have anatomical meaning and the Markov random field (MRF) model is used to find local spatial relationships between labeled structures. FS implements a model based on a mixture of a small number of Gaussians for each structure for each point in the space and maximum posterior estimate of the model parameters to assign one of the 37 ROI labels to each voxel [27]. FreeSurfer allows for manual editing of segmentation results; however, it is an extremely time-consuming procedure and McCarthy et al. [28] did not find significant differences between segmented volumes with and without manual corrections. The volumes of the ROIs used in this study have been extracted from the `aseg.stats` FS output [19].

SPM allows the segmentation of brain structural data in GM, WM and cerebrospinal fluid (CSF), and implements a variety of processing algorithms and statistical functions to make voxel-wise group analyses. The SPM analysis pipeline is shown in Fig. 2(b). Before segmenting the brain structures it needs to align the image on the anterior commissure to avoid possible segmentation algorithm failure. The `spm_preproc_run` script allows the segmentation into different tissue classes, using a modified Gaussian Mixture Model. It includes three steps: 1) non-uniformity intensity correction; 2) registration to the tissue probability maps representing the prior probability of different tissue classes; 3) posterior

1 probability computation using Bayes model to combine the prior probability with the tissue type probabilities derived
2 from voxel intensities. It is a circular process that includes classification, bias correction and registration treads [29]. To
3 mitigate the effect of partial volume it is appropriate to set the number of Gaussians to 2 for each tissue since a voxel
4 could contain a signal from a number of different tissues [18]. To preserve the total amount of GM and WM the
5 modulation operation is applied, in order to correct for regional enlargement/shrinkage of the volumes during spatial
6 normalization, the warped images are multiplied, voxel-by-voxel, with the relative volumes of tissue (i.e. the Jacobian
7 determinants of the deformations). To segment the subcortical structures for this study (hippocampus, putamen, caudate
8 and brainstem) an extension of SPM has been considered, implementing the atlas Neuromorphometric labels [17],
9 which can be used to mask GM and WM probability maps. Brain tissues volumes were obtained by using the
10 *spm_get_volumes* script [8].

11 We extracted the brain tissue volumes (GM, WM) and subcortical structures volumes (hippocampus, putamen, caudate,
12 brainstem) obtained with SPM and FS for all the subjects of both data samples, and we used these values to carry out
13 the repeatability and reproducibility analyses.

20 **Repeatability, reproducibility and bias measures**

21 Firstly, we quantified the intra-method repeatability of each method in estimating brain structures volume through a
22 test-retest analysis. Secondly, we evaluated the inter-method reproducibility of estimated volumes comparing the two
23 processing methods. These analyses were conducted in parallel for the two available data samples.

24 To evaluate the intra-method repeatability, we first computed the Pearson's correlation between the volumes obtained
25 for each brain structure of each subject in the test and retest scans; then, to quantify the agreement we implemented the
26 Bland-Altman (BA) plot representation [30], reporting the percentage differences between test and retest measures for
27 each subject. In this plot, for each pair the percentage difference of the two measurements $\left(\frac{V_{scan}-V_{rescan}}{\frac{V_{scan}+V_{rescan}}{2}}\right)*100$ is

28 reported as a function of the average measured volume $\frac{V_{scan}+V_{rescan}}{2}$, together with the mean (d) of this average
29 percentage difference and the limits of 95% confidence interval (C.I.) agreement.

30 We checked the normality of the distribution of the differences with the Shapiro-Wilk test. We used Bland-Altman plots
31 to detect possible systematic biases between test and retest scans. The test-retest measured volumes can be considered
32 equal if the percentage difference is null within the limits of agreements.

33 To evaluate the inter-method reproducibility, we used the brain structures volumes obtained in the segmentation of the
34 first set of scans, for each dataset separately. We computed Pearson's correlation between the volume measures
35 obtained with the two different software. This analysis was performed for both datasets. In addition, to estimate possible
36 systematic differences between the segmented volumes with the two different methods, we implemented the BA plot
37 representation.

38 **A practical example of between-group comparison**

39 To investigate whether the use of the two different preprocessing pipelines (SPM12 and FS v6.0) has a direct impact on
40 the results of a neuroscience study, we compared the brain volume measures obtained with each software for the male
41 and female subsamples, in order to reveal gender-related volume differences [11,16,31–33].

42 For each method, we tested male-female differences in all brain volumes on both datasets with t-test and calculated the
43 effect sizes, Cohen's d [34] as:

$$d = \frac{M_{male} - M_{female}}{SD_{pooled}}$$

$$SD_{pooled} = \sqrt{\frac{(n_{male}-1)\sigma_{male}^2 + (n_{female}-1)\sigma_{female}^2}{(n_{male}+n_{female}-2)}}$$

Possible variations in the shape of the segmented regions have been quantified in terms of the Dice (D) similarity index, which is an overlap measure between two binary images, defined as:

$$D = \frac{2|A \cap B|}{|A| + |B|}$$

and ranging from 0 to 1. A Dice index equal to 0 means that there is no overlap, whereas D equals to 1 means that the overlap is perfect [35]. To compare SPM and FS segmented volumes, the SPM tissues probability maps were binarized using a 0.5 threshold. We visually verified that brain masks derived using such thresholds were more accurately defined than by using other values [36].

By contrast, FS segmented ROIs are already provided as binary masks. The spatial comparison has been carried out in the native space of the images. Thus, it was necessary to transform back to the native space the segmented ROI maps for both methods. For FS we used the library function ‘*mri_label2vol*’, which converts a label mask into a mask in the native space [19]. For SPM we transformed back to the native space the brain masks using the ‘*spm_normalize_to_write*’ and the ‘*spm_realign*’ scripts [17].

Results

Intra-method Repeatability

Pearson’s correlations between the volumes obtained on test and retest MRI data are reported in Table 2 for both Kirby and OASIS data samples. SPM showed high Pearson’s correlation values on both data samples (r in the 0.98-0.99 range for GM, MW and in the four considered subcortical regions). FS showed high values of r on the Kirby dataset (r in the 0.98-0.99 range for GM and MW, r in the 0.95-0.99 range for the four subcortical regions). We also reported in Table 2 the average percentage differences (d) between test-retest volumes, their standard deviation (s) over the sample and the limits of agreement corresponding to the 95% C.I. in the measure of d for both SPM and FS on the Kirby and OASIS data samples.

The Bland-Altman plots are shown in Figs. 3-4 for GM and WM. The BA plots for the subcortical volumes are provided in the Supplementary Material.

The mean percent differences for SPM are always consistent with zero, showing that the volume estimates are repeatable, whereas for FS this consideration is true in all comparisons except for the GM and WM volumes obtained on the OASIS database. For these quantities the test measures are systematically higher, $d = (4.6 \pm 1.3) \%$ and lower $d = (-2.8 \pm 1.2) \%$ than the retest measures, respectively.

Inter-method reproducibility

The inter-method reproducibility analysis has been conducted on the measures obtained from the first scan for each data sample. Bar plots of the volumes for the six ROIs are shown in Fig. 5(a) and 5(b) for Kirby and OASIS data

1 samples, respectively. In Table 3 we report the Pearson's correlations between SPM and FS measures, as well as
2 the percentage differences (d) averaged over the subjects, their standard deviations (s) and the 95% C.I. limits on d.
3 The Bland-Altman plots obtained with the measures of the Kirby and OASIS data samples are reported in Figs. 6
4 and 7 for GM and WM, respectively. The BA plots for the subcortical volumes are provided in the Supplementary
5 Material. The Pearson's correlation coefficients are above 0.8 for all measures on both Kirby and OASIS data
6 samples, except for the hippocampus ($r=0.72$ on Kirby and $r=0.78$ on OASIS). The Bland-Altman plots show
7 systematic biases: SPM provides a significantly greater volume of GM and significantly lower volumes of WM
8 and the subcortical ROIs with respect to FS.
9

10 These findings are consistently detected on both Kirby and OASIS data samples. Dice's similarity coefficients
11 between SPM and FS segmentations for each brain structure are reported in Table 3. Dice values are in the 0.76-
12 0.83 range. Consistently on both data samples, the smaller structures (hippocampus, putamen and caudate) show
13 the worst overlap, generally below 0.8, whereas brain tissues (GM and WM) and the brainstem show Dice values
14 generally above 0.8. The modest overlap of segmented structures ($D<0.8$) occurs in particular in ROIs with poor
15 contrast or difficulties in the boundary definition between GM and WM matter, such as those reported in Fig. 8
16 (putamen, caudate and hippocampus). Fig. 9 shows the overlay of the GM masks obtained with SPM and FS,
17 where the difference in the definition of the brain regions belonging to the GM is clearly visible. For example, the
18 thalamus is not included in the GM tissue identified by SPM. We reported the overlay of the ROI masks obtained
19 by SPM and FS, for the worst cases of the Kirby and the OASIS data samples, respectively in Figs. 10 and 11.
20
21
22
23
24
25
26
27

28 **Consistency test of male vs. female volume comparison**

29 The two-sample t-test between volume measures of the male and female subgroups obtained with SPM12 and FS v6.0
30 consistently revealed significant gender-related differences on the Kirby data sample. In that case, the Cohen's d effect
31 sizes [34] range from 0.76 (large) to 0.84 (huge) for both FS and SPM (see Table 4 and Fig. 12). By contrast, gender-
32 related differences appear subtler on the OASIS data sample, and no statistically significant differences are actually
33 detected for the global WM and for the hippocampus, caudate and brainstem volume measures, consistently for SPM
34 and FS (see Table 4 and Fig. 13). Among the subcortical structures, only the putamen volume is found to be
35 significantly larger in the male cohort and with very large Cohen's d values consistently for both segmentation methods.
36 A relevant inconsistency between the two different segmentation methods was found for the GM volume. In fact, a
37 significantly larger GM volume is found for the male cohort with a large Cohen's d according to FS measures, while the
38 analysis of the SPM GM measure does not confirm this finding.
39
40
41
42
43
44
45
46

47 **Discussion**

48 We examined the intra- and inter-method agreement of two popular automatic brain MRI segmentation tools (SPM and
49 FS), using the publicly available Kirby and OASIS datasets, containing high-resolution structural MRI images of
50 healthy subjects. The choice of the methods and of the data samples makes this study reproducible and extendable by
51 other researchers.
52

53 Although extremely high Pearson's correlation coefficients between test and retest measures have been found for both
54 SPM and FS, the BA plots revealed very good repeatability of both methods only on the Kirby dataset. By contrast, on
55 the OASIS data sample, the BA analysis detected non-null biases for the FS measures: for example, for GM and WM d
56 = 4.6 % and $d= -2.7$ % respectively. On the contrary, SPM showed no or smaller bias on them ($d = 0.1$ % and $d= -0.5$ %
57 for GM and WM respectively).
58
59
60
61
62
63
64
65

1 The OASIS dataset presents several differences with respect to the Kirby dataset. First of all, there is a significant
2 average time between test-retest is about three weeks (while Kirby retest acquisitions are made in the same day).
3 However, a reduction of the GM close to 5% is not likely in this time-lapse, and a simultaneous increase of the WM
4 close to 3% is definitely unrealistic. Another difference between the two datasets is the field strength (3T for Kirby and
5 1.5 for OASIS). Regarding this point, literature reports consistency in volume estimation at 1.5T and 3T, for both FS
6 and SPM [37]. Eventually, it is not possible to exclude the existence of differences in the populations underlying the
7 two datasets (for example, the mean age in Kirby is 32 ± 9 and 23.4 ± 3.9 in OASIS). However, the subjects are healthy
8 volunteers in both datasets and a significant difference in brain volumes is not expected.

9 These considerations lead us to conclude that SPM is more robust with respect to any variation that may have occurred
10 between test and retest scans on that data sample.

11 It is worth noticing that on both data samples the standard deviations of the test-retest percent volume differences are
12 generally higher when using FS, indicating that small differences in patient's orientations due to repositioning may have
13 a greater effect on FS than on SPM measures.

14 The inter-method reproducibility analysis revealed discrepancies between the volumes calculated by SPM and FS.
15 These discrepancies are visible both in the BA plots and in terms of the Dice indices. Larger values have been
16 systematically found by FS for the WM and the four subcortical ROIs with respect to SPM. By contrast, the GM
17 volume estimated by FS is lower with respect to the one estimated by SPM. Of note, one recently published study [38]
18 found that SPM12 overestimates the segmented volumes, in line with our results. Indeed, their results suggest that
19 FreeSurfer cortical thicknesses were lower compared to SPM12 values. These differences in the definition of the
20 boundary between GM and WM can be due to the implementation of different segmentation algorithms in SPM and FS,
21 including the adoption of different reference atlases (ICBM-452 [35] T1 brain atlas in SPM12 [17] and MNI 305 [39] in
22 FS).

23 The Dice indices highlighted an overlap between the ROIs segmented with the two methods of about 80%, with lower
24 values in case of subcortical ROIs. This result, which is consistently found on both data samples, can be understood in
25 terms of the larger surface-to-volume ratio of smaller structures. In fact, smaller structures are more prone to
26 segmentation discrepancies due to the different definitions of the boundary between GM and WM by the two
27 algorithms. Additional sources of discrepancy in segmenting subcortical structures are provided by the arbitrariness in
28 some cases in defining their boundaries with respect to surrounding structures, as the case of the hippocampus and the
29 confining amygdala.

30 To test for possible inconsistencies in group comparison results due to the choice of different segmentation algorithms,
31 we set up a two-group comparison between the only subgroups available in this study, i.e. the male and female cohorts.
32 According to numerous studies [11,16,31–33], males are expected to have on average larger absolute brain volumes
33 with respect to females. This result has been confirmed by the analysis of brain volume features obtained both with FS
34 and SPM on the Kirby data sample. By contrast, on the OASIS data sample, this effect is not noticeable, except for one
35 of the subcortical ROIs, consistently for both SPM and FS calculated measures.

36 The only concerning inconsistency between the two methods we could identify with this case study is the significant
37 greater GM volume of the male cohort, obtained only in the analysis of the FS measures. This kind of inconsistent
38 findings, obtained by straightforward comparisons of the volume measures provided by two widely used segmentation
39 tools, can definitely affect the results of neuroimaging studies and their interpretation and lead to irreproducible results
40 in the literature.

1 Among the possible limitations of this study is the choice of the selected ROIs. With respect to segmented brain tissues,
2 we limited to GM and WM because the CSF is not provided by FS. The choice of the four subcortical regions
3 (hippocampus, putamen, caudate and brainstem) included both larger and smaller structures, characterized either by
4 different contrasts or by hardly defined borders with respect to surrounding tissues. Another possible limitation is the
5 quite small number of subjects available for each dataset (21 subjects for Kirby and 20 for OASIS). Nevertheless, these
6 data samples allowed identifying systematic intra- and inter-method discrepancies. In addition, this sample size
7 corresponds to the minimal dataset size generally adopted in research studies.

8
9
10 It was not possible to make an absolute evaluation of the accuracy of the segmentation methods, because no gold
11 standard segmentation is available for the data samples we analyzed.

12
13 Recently, with the introduction of artificial intelligence, research is heading towards new solutions [40,41] that have the
14 potential to overcome some limits that these approaches still present. Therefore, it could be useful to apply the
15 presented analysis also to the new machine learning-based segmentation algorithms.

16 17 18 19 **Conclusions**

20
21 This paper has provided a comparison between SPM and FS in terms of the intra-method repeatability and inter-method
22 reproducibility of ROI volumes, evaluated on two different data sets. The considerations above lead us to support SPM
23 as a more consistent tool to evaluate ROI volumes. In any case, as the two methods rely on different algorithm
24 pipelines, which can be differently affected by the presence of abnormalities, image artifacts, or variations in the
25 acquisition protocol parameters, we suggest to cross-validate the findings of each research study against different
26 segmentation methods before proceeding to their interpretation.

27 28 29 30 **Acknowledgments**

31
32 The OASIS project was funded by grants P50 AG05681, P01 AG03991, R01 AG021910, P50 MH071616, U24
33 RR021382, R01 MH56584.

34
35 This work has been partially funded by the Tuscany Government (Bando FAS Salute by Sviluppo Toscana,
36 ARIANNA Project), and by the National Institute of Nuclear Physics (nextMR project).

37
38 Conflict of Interest Statement: The authors declare that the research was conducted in the absence of any
39 commercial or financial relationships that could be construed as a potential conflict of interest.

40 41 42 43 **References**

- 44
45
46
47 [1] Hogan RE, Mark KE, Choudhuri I, Wang L, Joshi S, Miller MI, et al. Magnetic Resonance Imaging
48 Deformation-Based Segmentation and Temporal Lobe Epilepsy 2000;13:217–8. doi:10.1053/jdim.2000.6897.
49
50 [2] Sachdeva J, Kumar V, Gupta I, Khandelwal N, Ahuja CK. Segmentation, feature extraction, and multiclass
51 brain tumor classification. J Digit Imaging 2013;26:1141–50. doi:10.1007/s10278-013-9600-0.
52
53 [3] Akhil M, Aishwarya R, Lal V, Mahesh S. Comparison and evaluation of segmentation techniques for brain mri
54 using Gold Standard. Indian J Sci Technol 2016;9. doi:10.17485/ijst/2016/v9i46/106495.
55
56 [4] Maclaren J, Han Z, Vos SB, Fischbein N, Bammer R. Reliability of brain volume measurements: A test-retest
57 dataset. Sci Data 2014;1:1–9. doi:10.1038/sdata.2014.37.
58
59 [5] Chard DT, Parker GJM, Griffin CMB, Thompson AJ, Miller DH. The reproducibility and sensitivity of brain
60 tissue volume measurements derived from an SPM-based segmentation methodology. J Magn Reson Imaging
61
62
63
64
65

2002;15:259–67. doi:10.1002/jmri.10064.

- [6] Selgrade ES, Wagner HR, Huettel SA, Wang L, McCarthy G, Morey RA, et al. Scan-rescan reliability of subcortical brain volumes derived from automated segmentation. *Hum Brain Mapp* 2010;00:1751–62. doi:10.1002/hbm.20973.
- [7] Ochs AL, Ross DE, Zannoni MD, Abildskov TJ, Bigler ED, For the Alzheimer’s Disease Neuroimaging Initiative. Comparison of Automated Brain Volume Measures obtained with NeuroQuant® and FreeSurfer. *J Neuroimaging* 2015;25:721–7. doi:10.1111/jon.12229.
- [8] Katuwal GJ, Baum SA, Cahill ND, Dougherty CC, Evans E, Evans DW, et al. Inter-method discrepancies in brain volume estimation may drive inconsistent findings in autism. *Front Neurosci* 2016;10. doi:10.3389/fnins.2016.00439.
- [9] Wenger EI, Mårtensson J, Noack H, Bodammer NC, Kühn S, Schaefer S, Heinze HJ, Düzel E, Bäckman L, Lindenberger U LM. Comparing manual and automatic segmentation of hippocampal volumes: reliability and validity issues in younger and older brains. *2914:4236–48*. doi:10.1002/hbm.22473.
- [10] Kazemi K, Noorizadeh N. Quantitative Comparison of SPM, FSL, and Brainsuite for Brain MR Image Segmentation. *J Biomed Phys Eng* 2014;4:13–26.
- [11] Perlaki G, Orsi G, Plozer E, Altbacker A, Darnai G, Nagy SA, et al. Are there any gender differences in the hippocampus volume after head-size correction? A volumetric and voxel-based morphometric study. *Neurosci Lett* 2014;570:119–23. doi:10.1016/j.neulet.2014.04.013.
- [12] Battaglini M, Jenkinson M, De Stefano N. SIENA-XL for improving the assessment of gray and white matter volume changes on brain MRI. *Hum Brain Mapp* 2018. doi:10.1002/hbm.23828.
- [13] Perlaki G, Horvath R, Nagy SA, Bogner P, Doczi T, Janszky J, et al. Comparison of accuracy between FSL’s FIRST and Freesurfer for caudate nucleus and putamen segmentation. *Sci Rep* 2017;7:1–9. doi:10.1038/s41598-017-02584-5.
- [14] Tae WS, Kim SS, Lee KU, Nam EC, Kim KW. Validation of hippocampal volumes measured using a manual method and two automated methods (FreeSurfer and IBASPM) in chronic major depressive disorder. *Neuroradiology* 2008;50:569–81. doi:10.1007/s00234-008-0383-9.
- [15] Jorge Jovicich, Silvester Czanner, Xiao Han, David Salat, Andre van der Kouwe, Brian Quinn, et al. MRI-derived measurements of human subcortical, ventricular and intracranial brain volumes: reliability effects of scan sessions, acquisition sequences, data analyses, scanner upgrade, scanner vendors and field strengths. *Neuroimage* 2009;46:177–92.
- [16] Barnes J, Ridgway GR, Bartlett J, Henley SMD, Lehmann M, Hobbs N, et al. Head size, age and gender adjustment in MRI studies: A necessary nuisance? *Neuroimage* 2010;53:1244–55. doi:10.1016/j.neuroimage.2010.06.025.
- [17] Neuroimaging B members & collaborations of the WCFH. SPM, Statistical Parametric Mapping n.d. <http://www.fil.ion.ucl.ac.uk/spm>.
- [18] Ashburner J, Barnes G, Chen C, Daunizeau J, Moran R, Henson R, et al. SPM12 Manual The FIL Methods Group (and honorary members). *Funct Imaging Lab* 2013:475–1. doi:10.1111/j.1365-294X.2006.02813.x.
- [19] Imaging L for CNAAMC for BBF. FreeSurfer n.d. <https://surfer.nmr.mgh.harvard.edu>.
- [20] Fischl B. FreeSurfer. *Neuroimage* 2012. doi:10.1016/j.neuroimage.2012.01.021.
- [21] Landman BA, Huang AJ, Gifford A, Vikram DS, Lim IAL, Farrell JAD, et al. Multi-parametric neuroimaging reproducibility: A 3-T resource study. *Neuroimage* 2011;54:2854–66. doi:10.1016/j.neuroimage.2010.11.047.

- 1 [22] Marcus DS, Wang TH, Parker J, Csernansky JG, Morris JC, Buckner RL. Open Access Series of Imaging
2 Studies (OASIS): Cross-sectional MRI data in young, middle aged, nondemented, and demented older adults. *J*
3 *Cogn Neurosci* 2007;19:1498–507. doi:10.1162/jocn.2007.19.9.1498.
- 4 [23] NITRC. NeuroImaging Tools & Resources Collaboratory n.d. <https://www.nitrc.org/projects/multimodal>.
- 5 [24] NITRC. NeuroImaging Tools & Resources Collaboratory. n.d. <https://www.nitrc.org/projects/oasis/>.
- 6 [25] Klein A, Tourville J. 101 Labeled Brain Images and a Consistent Human Cortical Labeling Protocol. *Front*
7 *Neurosci* 2012;6:1–12. doi:10.3389/fnins.2012.00171.
- 8 [26] Vaz S, Falkmer T, Passmore AE, Parsons R, Andreou P. The Case for Using the Repeatability Coefficient
9 When Calculating Test-Retest Reliability. *PLoS One* 2013;8:1–7. doi:10.1371/journal.pone.0073990.
- 10 [27] Fischl B, van Der Kouwe A, Salat DH, Busa E, Albert M, Dieterich M, et al. Whole brain segmentation:
11 automated labeling of neuroanatomical structures in the human brain. *Neuron* 2002;33:341–55.
12 doi:10.1016/S0896-6273(02)00569-X.
- 13 [28] Morey RA, Petty CM, Xu Y, Pannu Hayes J, Wagner HR, Lewis D V., et al. A comparison of automated
14 segmentation and manual tracing for quantifying hippocampal and amygdala volumes. *Neuroimage*
15 2009;45:855–66. doi:10.1016/j.neuroimage.2008.12.033.
- 16 [29] Ashburner J, Friston KJ. Unified segmentation. *Neuroimage* 2005;26:839–51.
17 doi:10.1016/j.neuroimage.2005.02.018.
- 18 [30] Myles PS, Cui J. I. Using the Bland–Altman method to measure agreement with repeated measures. *Br J*
19 *Anaesth* 2007;99:309–11. doi:10.1093/bja/aem214.
- 20 [31] Takahashi R, Ishii K, Kakigi T, Yokoyama K. Gender and age differences in normal adult human brain: Voxel-
21 based morphometric study. *Hum Brain Mapp* 2011;32:1050–8. doi:10.1002/hbm.21088.
- 22 [32] Ritchie SJ, Cox SR, Shen X, Lombardo M V., Reus LM, Alloza C, et al. Sex differences in the adult human
23 brain: Evidence from 5216 UK biobank participants. *Cereb Cortex* 2018;28:2959–75.
24 doi:10.1093/cercor/bhy109.
- 25 [33] Ruigrok ANV, Salimi-Khorshidi G, Lai MC, Baron-Cohen S, Lombardo M V., Tait RJ, et al. A meta-analysis
26 of sex differences in human brain structure. *Neurosci Biobehav Rev* 2014;39:34–50.
27 doi:10.1016/j.neubiorev.2013.12.004.
- 28 [34] Cohen J. *Statistical power analysis for the behavioral sciences*, second edition. 1988. doi:10.1234/12345678.
- 29 [35] Taha AA, Hanbury A. Metrics for evaluating 3D medical image segmentation: Analysis, selection, and tool.
30 *BMC Med Imaging* 2015;15. doi:10.1186/s12880-015-0068-x.
- 31 [36] Tudorascu DL, Karim HT, Maronge JM, Alhilali L, Fakhran S, Aizenstein HJ, et al. Reproducibility and bias in
32 healthy brain segmentation: Comparison of two popular neuroimaging platforms. *Front Neurosci* 2016;10:1–8.
33 doi:10.3389/fnins.2016.00503.
- 34 [37] Heinen R, Bouvy WH, Mendrik AM, Viergever MA, Biessels GJ, De Bresser J. Robustness of automated
35 methods for brain volume measurements across different MRI field strengths. *PLoS One* 2016.
36 doi:10.1371/journal.pone.0165719.
- 37 [38] Seiger R, Ganger S, Kranz GS, Hahn A, Lanzenberger R. Cortical Thickness Estimations of FreeSurfer and the
38 CAT12 Toolbox in Patients with Alzheimer’s Disease and Healthy Controls. *J Neuroimaging* 2018;28:515–23.
39 doi:10.1111/jon.12521.
- 40 [39] Collins DL, Neelin P, Peters TM, Evans AC. Automatic 3d intersubject registration of mr volumetric data in
41 standardized talairach space. *J Comput Assist Tomogr* 1994. doi:10.1097/00004728-199403000-00005.
- 42
43
44
45
46
47
48
49
50
51
52
53
54
55
56
57
58
59
60
61
62
63
64
65

- 1
2
3 [40] Wachinger C, Reuter M, Klein T. DeepNAT: Deep convolutional neural network for segmenting
4 neuroanatomy. Neuroimage 2018. doi:10.1016/j.neuroimage.2017.02.035.
5
6
7
8
9
10
11
12
13 [41] Chen H, Dou Q, Yu L, Qin J, Heng P-A. VoxResNet: Deep voxelwise residual networks for brain segmentation
14 from 3D MR images. Neuroimage 2018. doi:10.1016/j.neuroimage.2017.04.041.
15
16
17
18
19
20
21
22
23
24
25
26
27
28
29
30
31
32
33
34
35
36
37
38
39
40
41
42
43
44
45
46
47
48
49
50
51
52
53
54
55
56
57
58
59
60
61
62
63
64
65

Table 1. Structural MRI studies on the repeatability assessment of automatic segmentation methods

| Reference | Brain regions | Methods |
|--------------------------|---|---------------------------|
| Chard et al. (2002) | Gray Matter, White Matter | SPM99 |
| Jovicich et al. (2009) | Hippocampus, Thalamus, Caudate, Putamen, Pallidum, Amygdala, Lateral Ventricles, Inferior Lateral Ventricles, Intracranial | FS 4.0 |
| Katuwal et al. (2016) | Gray Matter, White Matter, Cerebrospinal fluid, Total intracranial volume | SPM8, FSL 5.0.4, FS 5.3 |
| Kazemi et al. (2014) | Gray Matter, White Matter, Cerebrospinal Fluid | SPM8, FSL 4.1, Brainsuite |
| Lehmann et al. (2010) | Hippocampus, Amygdala, Entorhinal cortex, Fusiform gyrus, Parahippocampal gyrus, Medial–inferior temporal gyrus, Superior temporal gyrus, Temporal lobe, Ventricles | FS 4.0.3 |
| Maclaren J et al. (2014) | Hippocampus, Lateral ventricles, Amygdala, Putamen, Pallidum, Caudate, Thalamus, Cerebral White Matter | FS 5.1 |
| Morey RA et al. (2010) | Amygdala, Brain Stem, Hippocampus, Lateral Ventricles, Nucleus Accumbens, Caudate, Putamen, Pallidum, Thalamus | FSL-FIRST 1.2, FS 4.5 |
| Ochs et al. (2015) | Total intracranial volume, Whole brain parenchyma, Cortical gray matter, Lateral ventricle, Inferior lateral ventricle, 3 rd ventricle, 4 th ventricle, Total cerebrospinal fluid, Caudate, Putamen, Pallidum, Thalamus, Amygdala, Hippocampus, Ventral diencephalon, Cerebellar white matter, Cerebellar gray matter, Cerebellum, Brain Stem | FS 5.3, NeuroQuant. 1.4 |
| Perlaki et al. (2017) | Caudate, Putamen | FSL 5.0.7, FS 4.5, FS 5.3 |
| Tae WS et al. (2008) | Hippocampus | FS 3.0.4, IBASPM (SPM2) |
| Wenger et al. (2014) | Hippocampus | FS 5.3 |

Table 2. Intra-method repeatability measurements for SPM and FS evaluated on the Kirby and OASIS data samples: Pearson's correlation and Bland-Altman plot parameters, e.g. mean (d) and standard deviation (s) of percent difference and limits of agreement corresponding to the 95% C.I. in volume difference.

| Kirby dataset | | | | | | | | |
|---------------|-----------------------|-------|-------|---------------------|-----------------------|-------|-------|---------------------|
| Brain region | SPM | | | | FS | | | |
| | Pearson's correlation | d (%) | s (%) | Limits of agreement | Pearson's correlation | d (%) | s (%) | Limits of agreement |
| GM | 0.99 | 0 | 1.1 | -2.2 to 2.1 | 0.98 | 1.0 | 2.0 | -2.9 to 5.0 |
| WM | 0.99 | 0 | 0.8 | -1.6 to 1.5 | 0.98 | -0.7 | 1.8 | -4.2 to 2.8 |
| Hippocampus | 0.99 | -0.2 | 0.7 | -1.5 to 1.2 | 0.95 | -1 | 3 | -7 to 6 |
| Putamen | 0.99 | -0.3 | 1.7 | -3.6 to 3.0 | 0.99 | -0.4 | 1.7 | -3.9 to 3.0 |
| Caudate | 0.99 | -0.1 | 0.8 | -1.8 to 1.5 | 0.99 | 0 | 1.5 | -2.8 to 2.9 |
| Brainstem | 0.99 | -0.4 | 0.7 | -1.7 to 1.0 | 0.99 | 0.2 | 1.5 | -2.8 to 3.2 |

| OASIS dataset | | | | | | | | |
|---------------|-----------------------|-------|-------|---------------------|-----------------------|-------|-------|---------------------|
| Brain region | SPM | | | | FS | | | |
| | Pearson's correlation | d (%) | s (%) | Limits of agreement | Pearson's correlation | d (%) | s (%) | Limits of agreement |
| GM | 0.99 | 0.1 | 1.4 | -2.7 to 2.9 | 0.99 | 4.6 | 1.3 | 2.1 to 7.1 |
| WM | 0.99 | -0.5 | 1.3 | -2.9 to 1.9 | 0.99 | -2.8 | 1.2 | -5.1 to -0.5 |
| Hippocampus | 0.98 | -1.3 | 0.8 | -2.8 to 0.2 | 0.96 | -2.7 | 2.0 | -6.6 to 1.2 |
| Putamen | 0.98 | 3.1 | 3.0 | -2.7 to 8.9 | 0.98 | 1.0 | 2.6 | -4.0 to 6.1 |
| Caudate | 0.99 | 0.7 | 1.3 | -1.9 to 3.2 | 0.99 | 1.2 | 2.1 | -2.9 to 5.2 |
| Brainstem | 0.99 | -0.1 | 1.7 | -3.5 to 3.3 | 0.99 | -0.5 | 2.3 | -5.0 to 3.9 |

Table 3. Inter-method reproducibility measurements between SPM and FS evaluated on the Kirby and OASIS data samples: Pearson's correlation; Bland-Altman parameters e.g. mean (d) and standard deviation (s) of percent difference and limits of agreement corresponding to the 95% C.I. in volume difference; Dice indices (D).

| Kirby dataset | | | | | |
|---------------|-----------------------|-------|-------|---------------------|-------------|
| Brain region | Pearson's correlation | d (%) | s (%) | Limits of agreement | D |
| GM | 0.94 | 11 | 3 | 4 to 17 | 0.80 ± 0.03 |
| WM | 0.98 | -13 | 2 | -10 to -17 | 0.81 ± 0.03 |
| Hippocampus | 0.72 | -21 | 6 | -34 to -8 | 0.78 ± 0.03 |
| Putamen | 0.86 | -34 | 5 | -24 to -45 | 0.76 ± 0.04 |
| Caudate | 0.80 | -23 | 8 | -39 to -8 | 0.80 ± 0.02 |
| Brainstem | 0.95 | -26 | 5 | -36 to -17 | 0.84 ± 0.02 |
| OASIS dataset | | | | | |
| Brain region | Pearson's correlation | d (%) | s (%) | Limits of agreement | D |
| GM | 0.96 | 13 | 3 | 9 to 18 | 0.83 ± 0.01 |
| WM | 0.95 | -11 | 3 | -17 to -5 | 0.83 ± 0.02 |
| Hippocampus | 0.78 | -17 | 5 | -28 to -7 | 0.78 ± 0.02 |
| Putamen | 0.84 | -34 | 6 | -47 to -22 | 0.77 ± 0.04 |
| Caudate | 0.93 | -23 | 6 | -35 to -11 | 0.79 ± 0.02 |
| Brainstem | 0.95 | -34 | 3 | -40 to -29 | 0.80 ± 0.02 |

Table 4. Gender differences in brain structures volumes of interest [ml] for SPM and FS evaluated on the Kirby and OASIS dataset: mean, standard deviation (SD) and statistic measures, t, p-value and Cohen's d.

*on p -value > 0.05

| Kirby dataset | | | | | | | | | | |
|---------------|----------|----------|--------------------|---------|-----------|---------|----------|--------------------|---------|-----------|
| Brain region | FS | | | | | SPM | | | | |
| | Mean±SD | | Statistic measures | | | Mean±SD | | Statistic measures | | |
| | Male | Female | t | p-value | Cohen's d | Male | Female | t | p-value | Cohen's d |
| GM | 677±34 | 590±57 | 4.0 | 0.001 | 1.9 | 744±32 | 663±59 | 3.7 | 0.002 | 1.7 |
| WM | 543±33 | 485±53 | 2.8 | 0.01 | 1.3 | 472±31 | 423±46 | 2.7 | 0.02 | 1.2 |
| Hippocampus | 8.7±0.7 | 7.9±0.7 | 2.4 | 0.02 | 1.1 | 7.1±0.3 | 6.4±0.5 | 3.5 | 0.003 | 1.6 |
| Putamen | 11±0.8 | 9.8±1.1 | 2.6 | 0.02 | 1.2 | 7.9±0.4 | 6.8±0.7 | 4.1 | 0.001 | 1.9 |
| Caudate | 7.6±0.8 | 6.7±0.8 | 2.5 | 0.02 | 1.2 | 6.0±0.4 | 5.3±0.5 | 3.3 | 0.004 | 1.5 |
| Brainstem | 22.4±1.6 | 18.6±2.7 | 3.7 | 0.002 | 1.7 | 17±1 | 14.5±1.8 | 3.6 | 0.003 | 1.7 |

| OASIS dataset | | | | | | | | | | |
|---------------|----------|----------|--------------------|---------|-----------|---------|----------|--------------------|---------|-----------|
| Brain region | FS | | | | | SPM | | | | |
| | Mean±SD | | Statistic measures | | | Mean±SD | | Statistic measures | | |
| | Male | Female | t | p-value | Cohen's d | Male | Female | t | p-value | Cohen's d |
| GM | 714±39 | 662±60 | 2.2 | 0.04 | 1.0 | 800±42 | 765±72 | 1.3 | 0.21* | 0.6 |
| WM | 528±35 | 513±63 | 0.6 | 0.53* | 0.3 | 482±34 | 456±53 | 1.3 | 0.22* | 0.6 |
| Hippocampus | 8.4±0.6 | 7.8±0.6 | 1.9 | 0.08 | 0.9 | 7.0±0.3 | 6.6±0.6 | 1.9 | 0.07 | 0.8 |
| Putamen | 11.5±0.9 | 10.2±1.1 | 2.8 | 0.01 | 1.3 | 8.0±0.5 | 7.2±0.9 | 2.3 | 0.03 | 1.0 |
| Caudate | 7.9±0.8 | 7.1±1.1 | 1.6 | 0.13* | 0.7 | 6.1±0.5 | 5.7±0.7 | 1.5 | 0.16* | 0.6 |
| Brainstem | 22.5±2.1 | 21.3±2.1 | 1.1 | 0.28* | 0.5 | 16±1 | 15.0±1.7 | 1.5 | 0.16* | 0.6 |

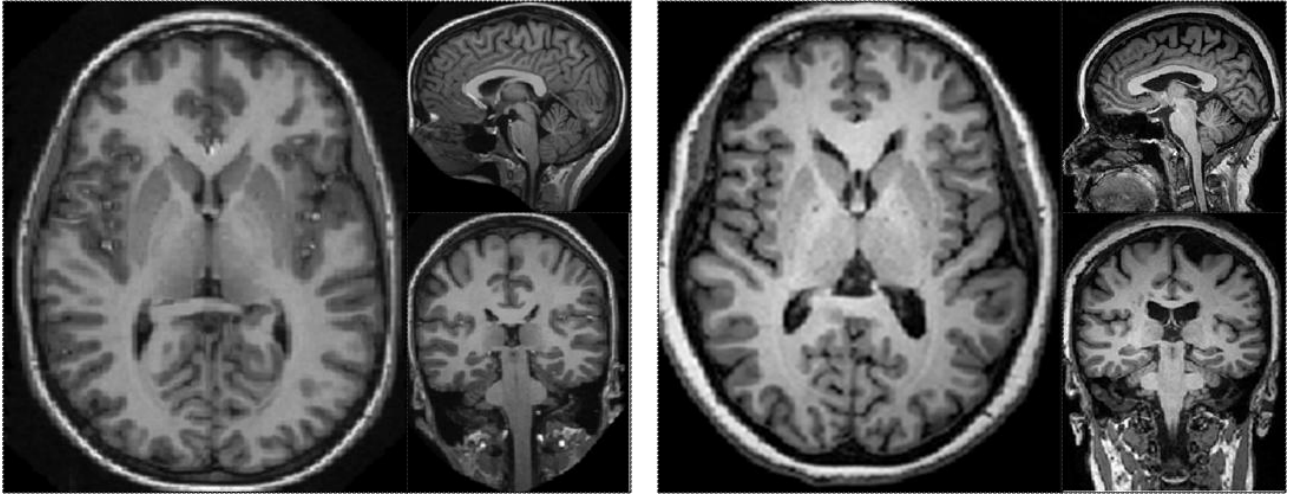


Fig. 1 Original axial, sagittal, coronal view of the 3D brain MRI data of two datasets OASIS (left) and Kirby-21 (right).

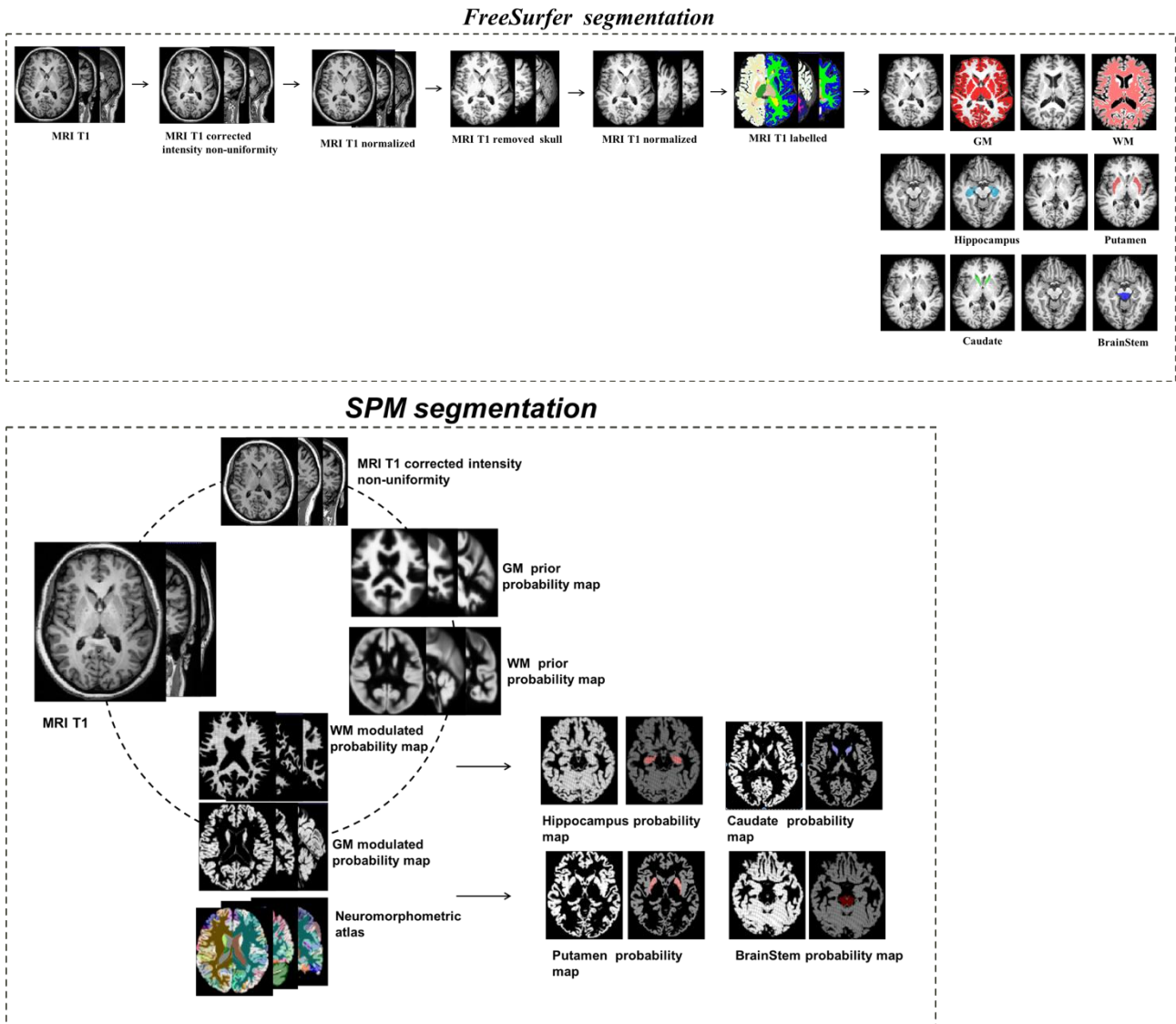


Fig. 2 (a) FreeSurfer analysis pipeline showing the main steps of interest from motion correction to automated subcortical segmentation; (b) SPM preprocessing pipeline, including also the use of the Neuromorphometric atlas.

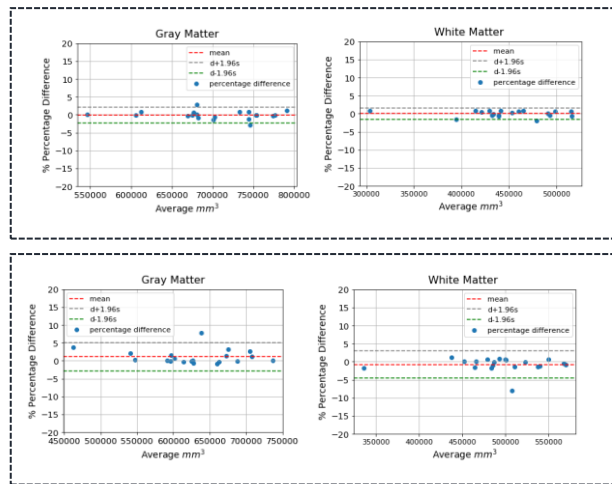


Fig. 3 Bland-Altman plots of segmented GM and WM by SPM (above) and by FS (below) in scan-rescan analysis on the Kirby-21 dataset. Bland-Altman plots of the four segmented subcortical structures are shown in the Supplementary Material.

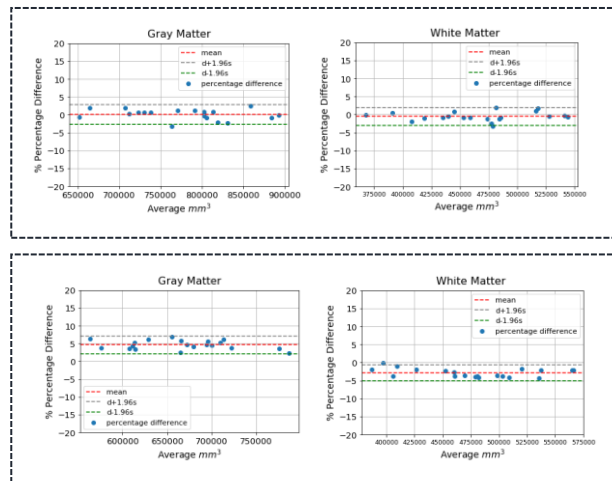


Fig.4 Bland-Altman plots of segmented GM and WM by SPM (above) and by FS (below) in scan-rescan analysis on the OASIS dataset. Bland-Altman plots of the four segmented subcortical structures are shown in the Supplementary Material.

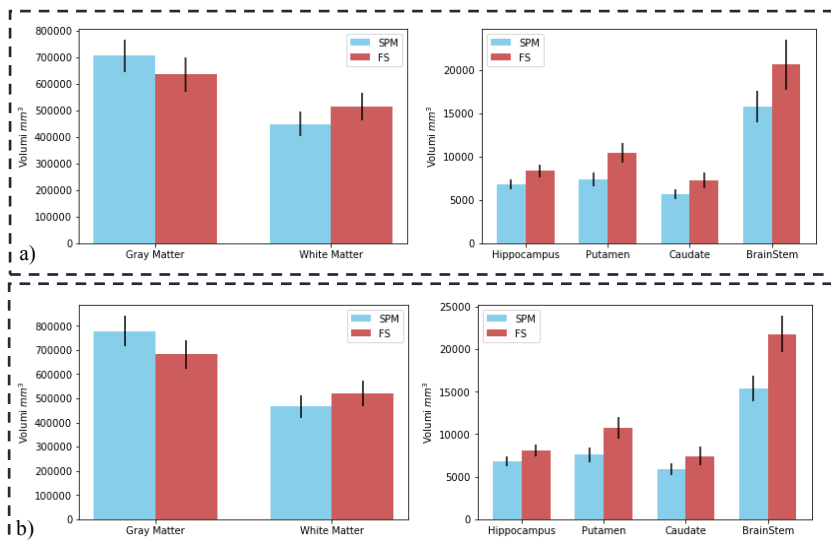


Fig. 5 Bar-plots of segmented brain tissues volumes and subcortical structures (a) on the Kirby-21 dataset, (b) on OASIS dataset.

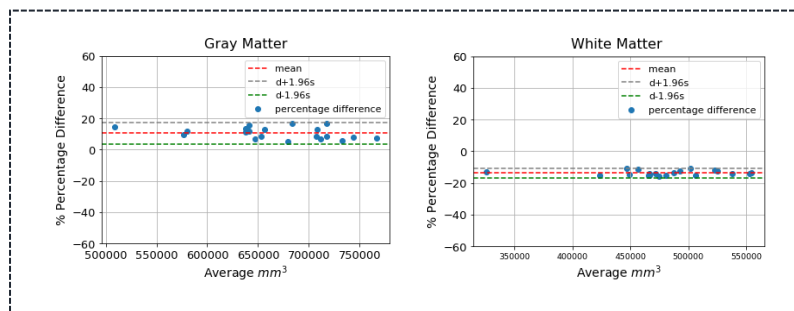


Fig. 6 Bland-Altman plots of segmented GM and WM by FS and SPM in the inter-method reproducibility analysis on the Kirby-21 dataset. Bland-Altman plots of the four segmented subcortical structures are shown in the Supplementary Material.

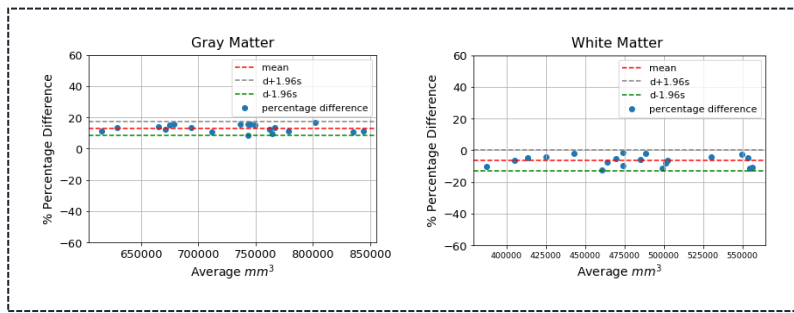


Fig. 7 Bland-Altman plots of segmented GM and WM by FS and SPM in the inter-method reproducibility analysis on the OASIS dataset. Bland-Altman plots of the four segmented subcortical structures are shown in the Supplementary Material.



Fig. 8 Highlight of the poor contrast and difficult of boundary definition for some subcortical anatomical structures for one example subject: zoom on the putamen and caudate area (left); zoom on the hippocampus area (right).

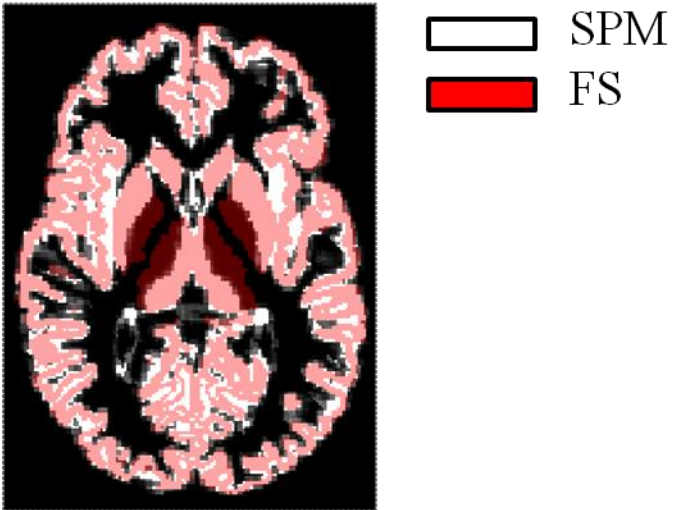


Fig. 9 GM ROI masks obtained with SPM (white) and FS (red). The difference in the definition of brain regions are clearly visible in the image (white: SPM; red: FS; pink: common regions). For example, the thalamus is not included in the GM tissue identified by SPM.

FS SPM

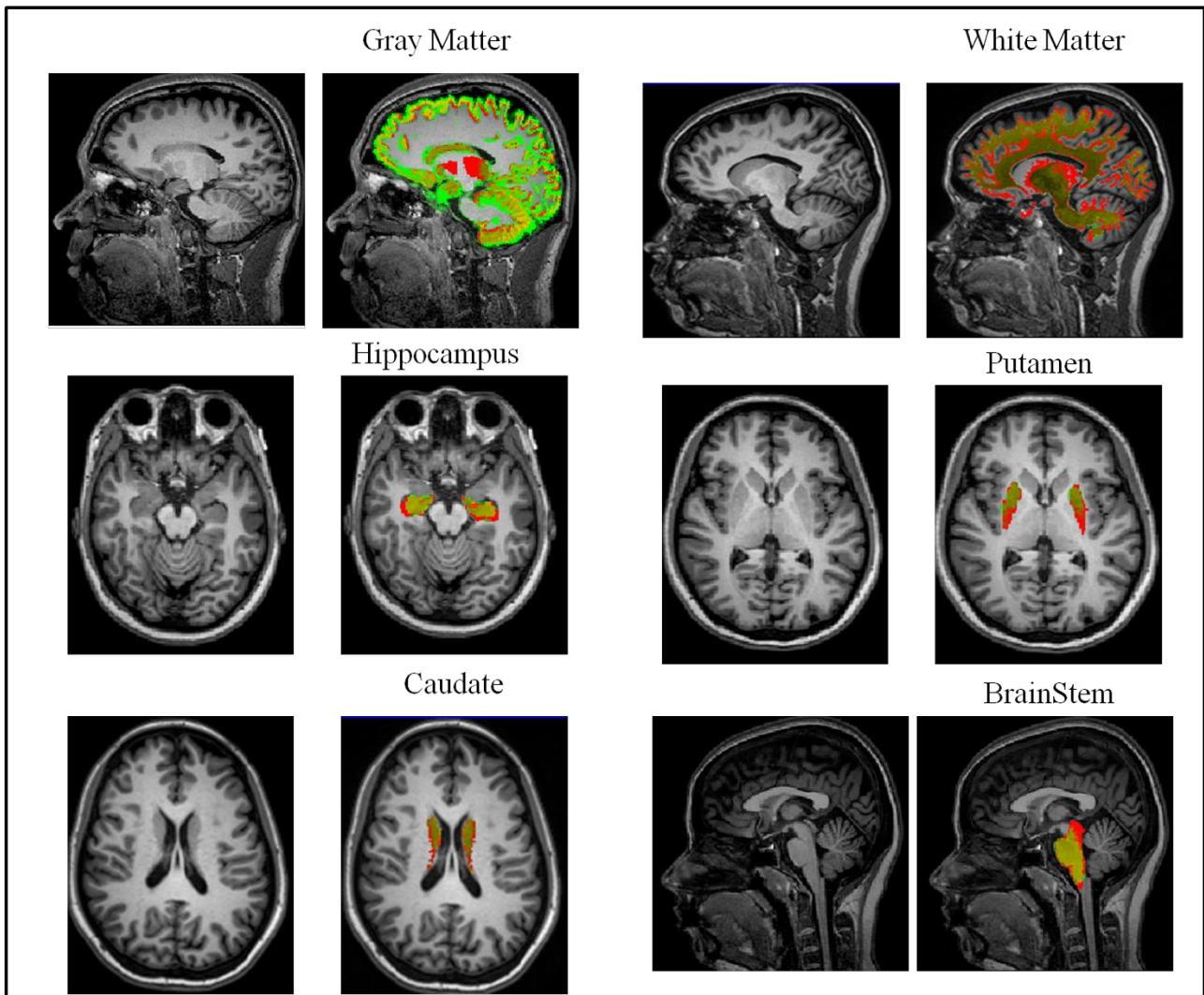


Fig.10 Overlay of segmented ROIs by SPM and by FS onto a single subject anatomical image in the native space for the worst case of the Kirby-21 data sample. GM and WM are visible on the first line; hippocampus and caudate on the second and third lines, respectively.

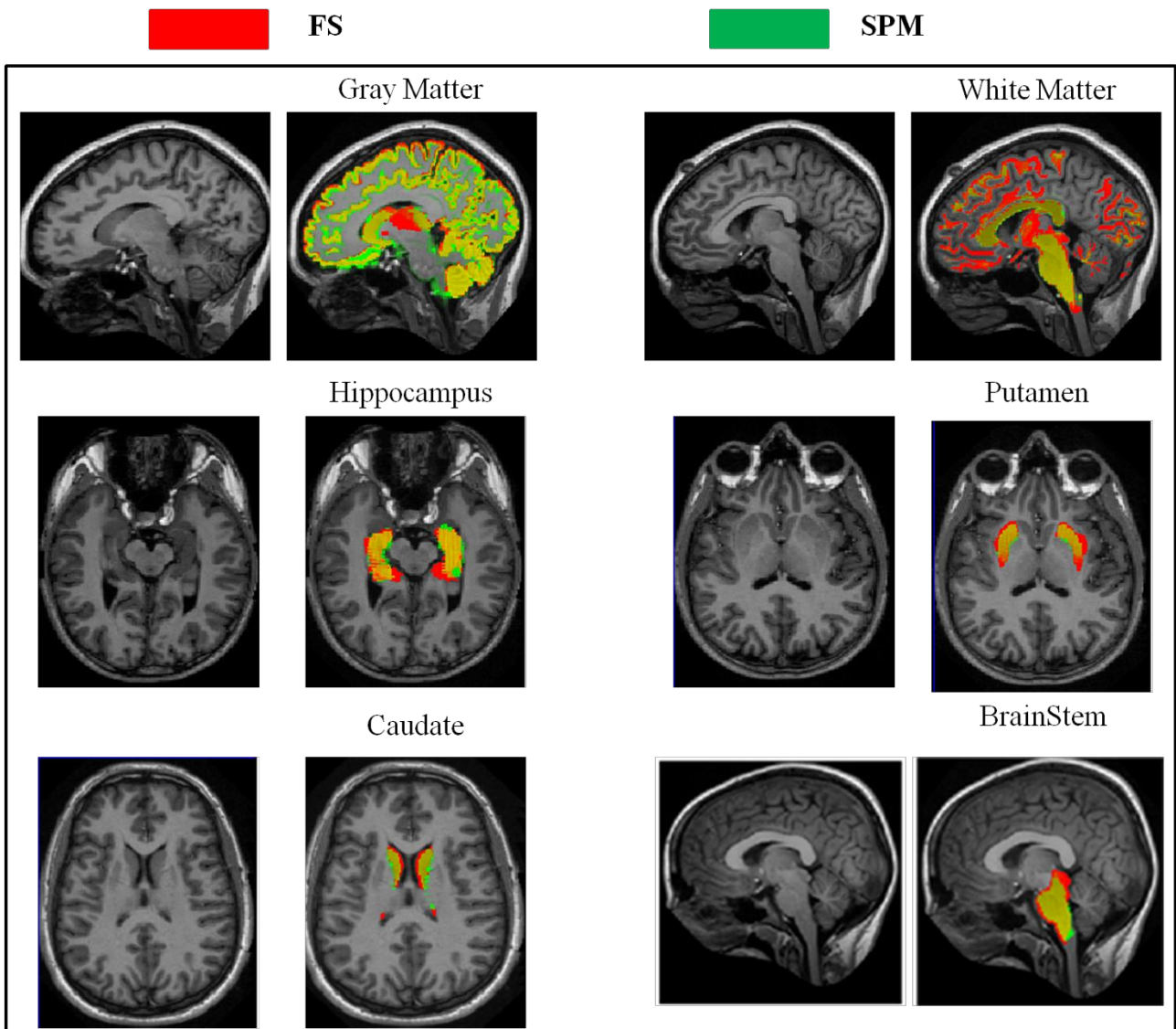


Fig. 11 Overlay of segmented ROIs by SPM and by FS onto a single subject anatomical image in the native space for the worst case of the OASIS data sample. GM and WM are visible on the first line; hippocampus and caudate on the second and third lines, respectively.

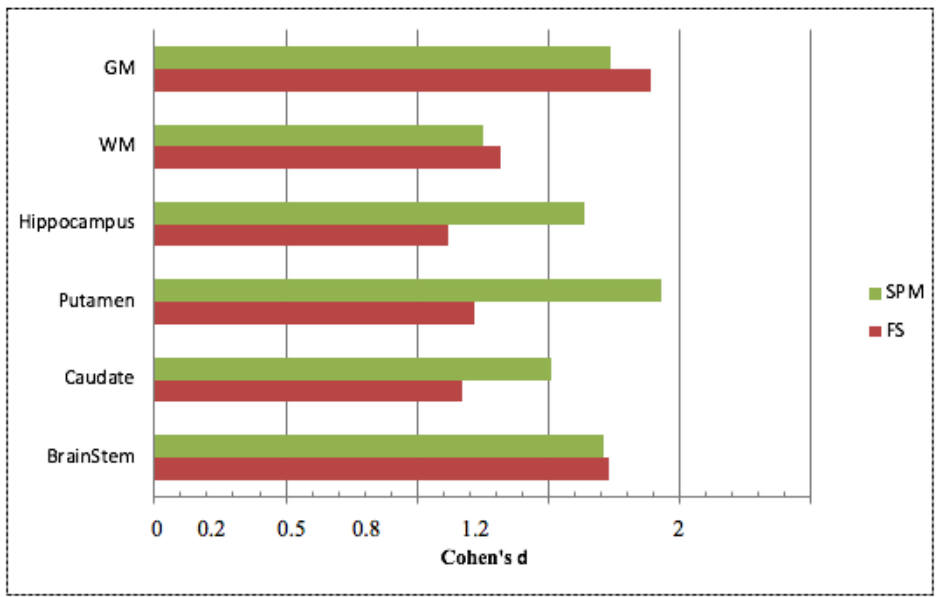


Fig. 12 Histograms of the Cohen's d effect sizes on the Kirby dataset. Green bars indicate the gender effect size obtained with SPM; red bars indicate the gender effect size obtained with FS.

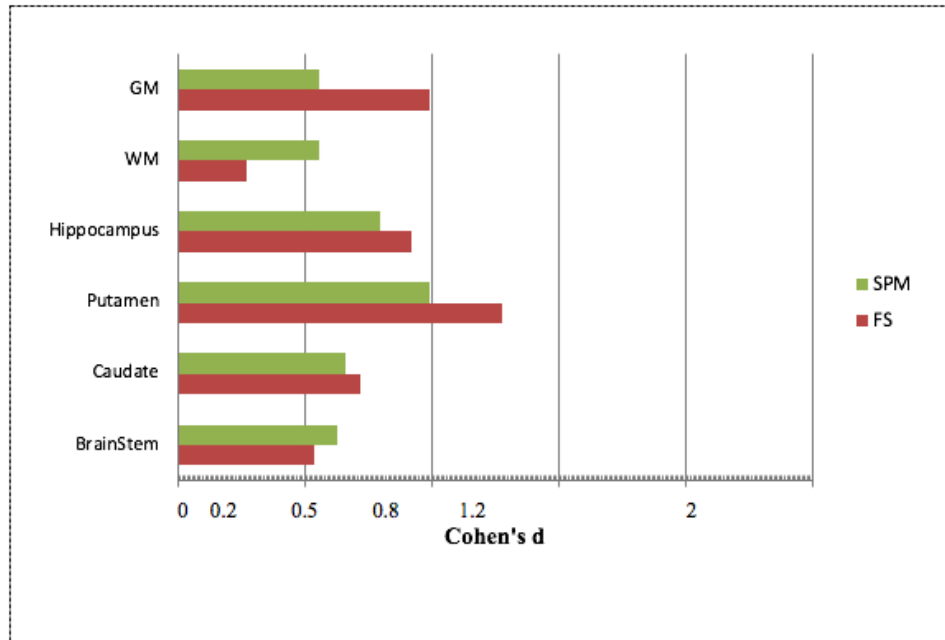


Fig. 13 Histograms of the Cohen's d effect sizes on the OASIS dataset. Green bars indicate the gender effect size obtained with SPM; red bars indicate the gender effect size obtained with FS.

Supplementary Material

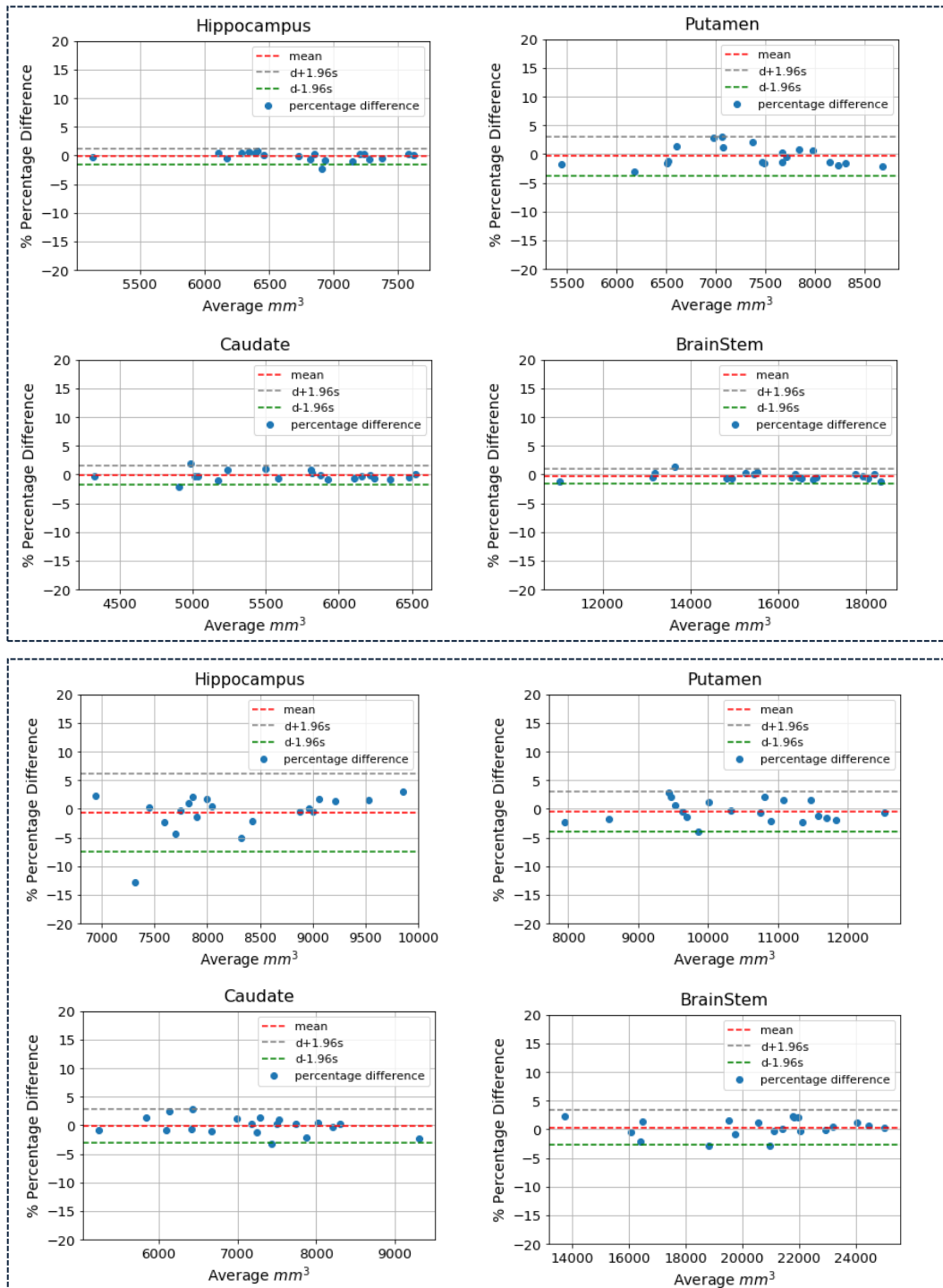


Fig.1s Bland-Altman plots of segmented subcortical structures by SPM (above) and by FS (below) in scan-rescan analysis on the Kirby-21 dataset.

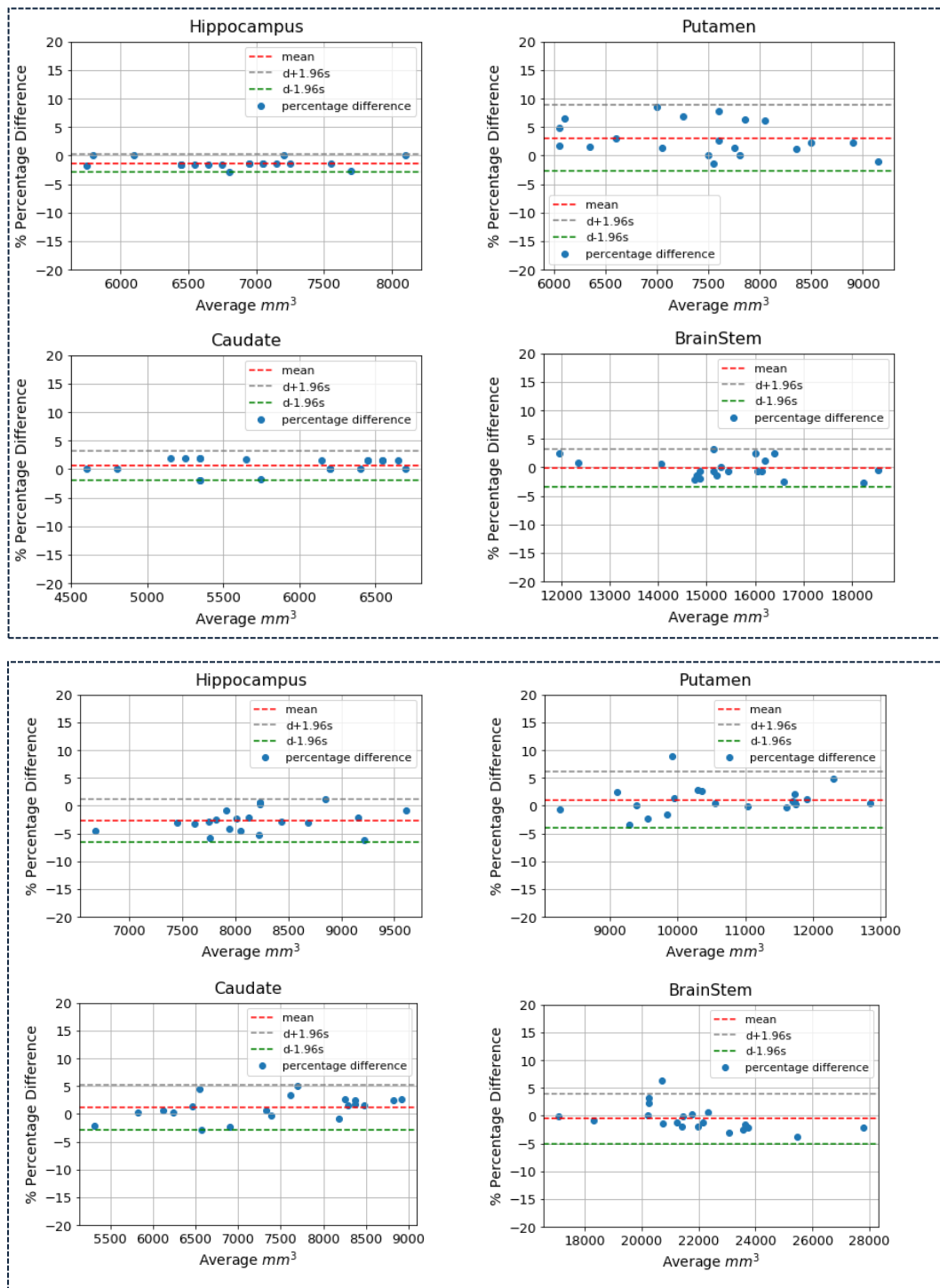


Fig. 2s Bland-Altman plots of segmented subcortical structures by SPM (above) and by FS (below) in scan-rescan analysis on the OASIS dataset.

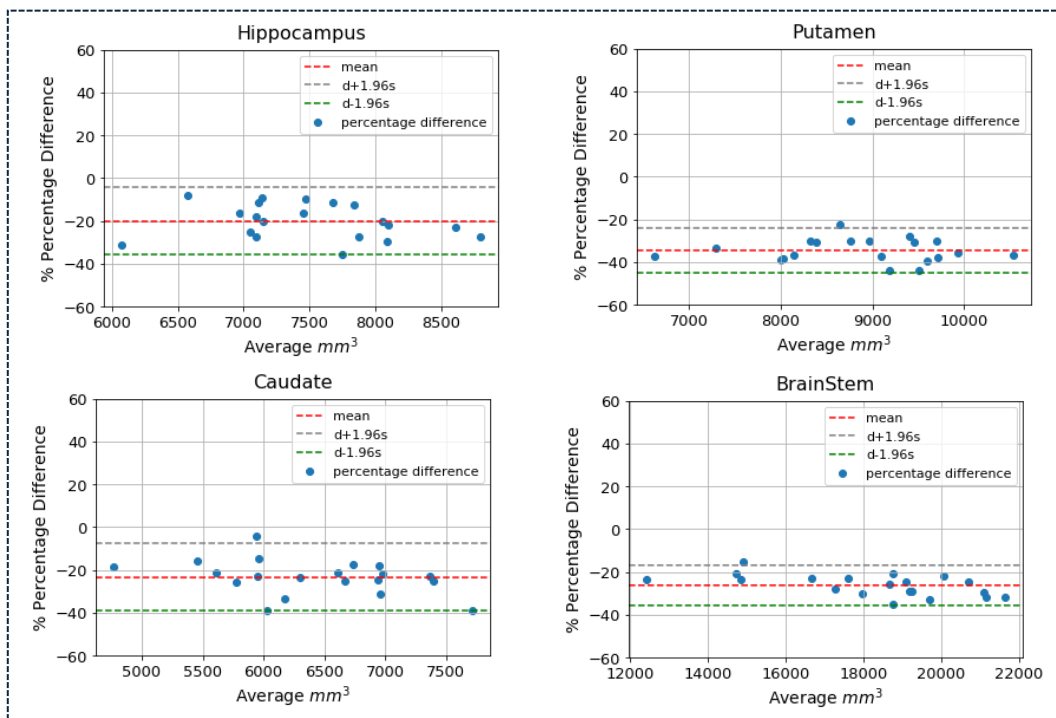


Fig. 3s Bland-Altman plots of segmented subcortical structures by FS and SPM in the inter-method reproducibility analysis on the Kirby-21 dataset.

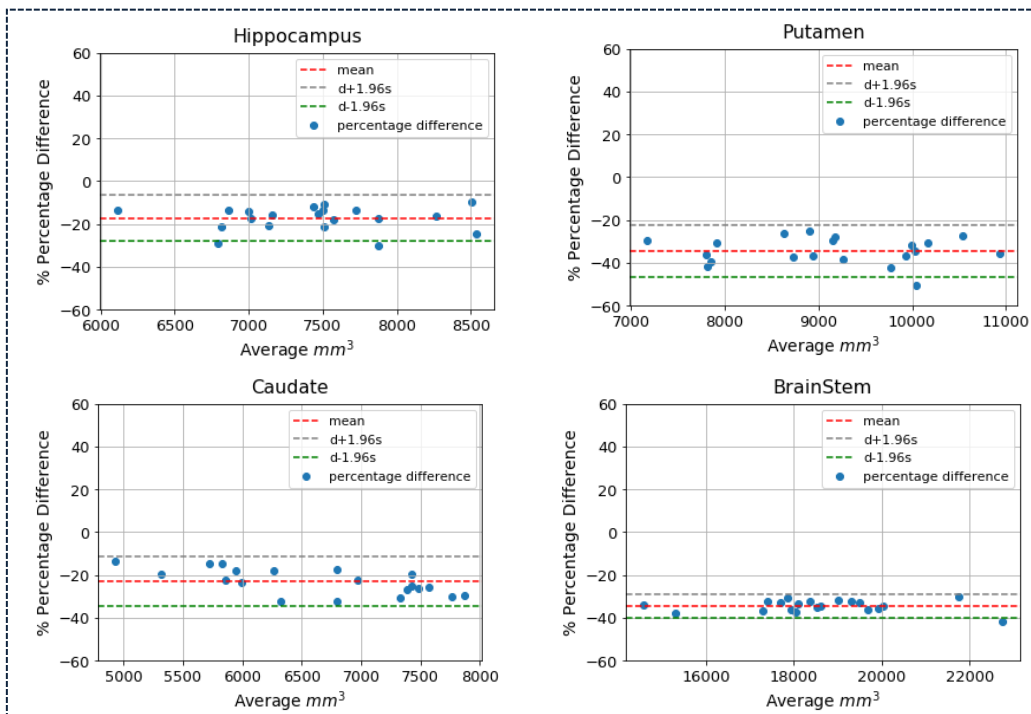


Fig. 4s Bland-Altman plots of segmented brain structures by FS and SPM in the inter-method reproducibility analysis on the OASIS dataset.